PROGRESS
IN COLOR, COLORANTS AND COATINGS

available online @ www.pccc.icrc.ac.ir

Progress in Color Colorants Coating 20 (2027), 1-12

Ministry of Science, Research and Technology
Institute for Color Science & Technology

A Ratiometric Naphthalimide-Based Fluorescent Chemosensor via Excimer-Monomer Switching for the Sensitive Detection of Copper (II) Ions

Sh. Rouhani
Department of Organic Colorants, Institute for Color Science and Technology, P.O. Box: 16765-654, Tehran, Iran

ARTICLE INFO

Article history:
Received: 17 Nov 2025
Final Revised: 28 Feb 2025
Accepted: 09 Mar 2026
Available online: 20 June 2026

Keywords:
Bifluorogenic
Copper ion
Naphthalimide
Diaza-18Crown 6

ABSTRACT

A newly designed diaza-18-crown-6 ether featuring two fluorogenic 1,8-naphthalimide side arms has been developed. This synthesized fluorescent dye (BNDA) presented a dual OFF-ON / ON-OFF response arising from switching between monomer and excimer emissions in the presence of copper ions. The binding behavior of BNDA with Cu^{2+} was thoroughly examined using fluorescence spectroscopy. The binding constant of BNDA with Cu^{2+} was determined through the Benesi–Hildebrand plot, yielding values of $5.57 \times 10^{6}\ M^{-1}$, indicating selective and sensitive interactions. This probe exhibited exceptional selectivity for copper ions, with a notably low detection limit of 29 nM, as well as a wide linear range of 2.9×10^{-4} – 4 µM response. To ascertain its practical application, BNDA was successfully applied for determining copper ions in real environmental samples of tap water, black tea, and human hair. Its good reversibility, stable response, and wide pH of 4.2 to 7.5, along with a strong linear range, make it a promising candidate for sensitive detection of Cu^{2+}. Prog Color Colorants Coat. 20 (2027), 1-12© Institute for Color Science and Technology.

1. Introduction

The developments of optical sensors have recently grown rapidly thanks to their possible applications in biotechnology, ecology, and medicine. Researchers are also interested in such sensors regarding cost, freedom from electrical interference, safety, possibility of remote sensing as well as real-time analysis. In recent years, several photo- and optometric sensors have been reported for selective determination of cationic and anionic species [1-3]. Over the past decade, optical chemosensors utilizing fluorescence sensing have emerged as significant research subjects owing to easy application, high selectivity, and sensitivity [1-9]. The interplay between recognition and signal reporting units continues to be a focal point in innovative optosensor design. Numerous photophysical processes and sensing mechanisms have been extensively reviewed in the literature, including intramolecular charge transfer (ICT), metal-ligand charge transfer (MLCT), photo-induced electron transfer (PET), resonance energy transfer (FRET), twisted intramolecular charge transfer (TICT), electronic energy transfer (EET), and excimer formation [3, 5]. The pursuit of ion sensing through fluorogenic materials has garnered substantial interest [7, 8, 10, 11].

Developing fluorescent chemosensors for detecting biologically or environmentally significant metal ions remains a critical research area. Copper ion levels need to be meticulously regulated in the human body given their cellular toxicity. Excess copper ions are used as a catalyst along the formation of reactive oxygen species (ROS), leading to damage. Elevated copper levels have been linked to several severe conditions, including Alzheimer's disease [12], Parkinson's disease, and Wilson's disease [13, 14].

Over recent decades, significant progress has been made in developing optical sensors for Cu^{2+} ions. Nevertheless, Cu^{2+} detection is often complicated by

*Corresponding author: * rouhani@icrc.ac.ir
https://doi.org/ 10.30509/pccc.2026.167724.1473

interference from other transition metal ions such as Co^{2+}, Ni^{2+}, Cr^{3+}, and Zn^{2+}. Thus, designing a specific fluorescent probe for Cu^{2+} remains a challenge. Selective chelation of macromolecules containing heteroatoms such as nitrogen, oxygen, and sulfur with metal ions is widely employed in chemical sensing. Crown ether derivatives that incorporate fluorescent moieties are especially promising for metal ion sensing through optical methods. Generally, crown ethers with oxygen hetero atoms are well-known for interacting with alkali-metal and alkaline-earth metal ions. When nitrogen replaces one or two oxygen donor atoms, aza crown ethers emerge as effective chelating ligands for transition metal cations. The binding affinity and selectivity of crown ethers is dependent on several factors, such as their size, charge density of the donor atoms, as well as the number of donor atoms. The nitrogen atom in the aza crown ether group acts as an electron donor, involves ICT and PET processes, along with cation complexation [15-17].

The design and application of colorants in advanced technologies has gained increasing importance in recent years [18]. 1,8-Naphthalimides have garnered attention in developing fluorescent molecular devices, including chemosensors [19-23], switching mechanisms, and logic operations [24-26]. 4-Amino-1,8-naphthalimides are noteworthy for their high emission intensity, large Stokes shift, and exceptional stability, making them suitable for various applications as chemosensing probes. Their strong electron-accepting properties and the potential for PET further enhance their utility.

Our research group has focused on designing and synthesizing 1,8-naphthalimide structures for fluorescence probes and chemosensor applications [27-30, 11]. Previously, we have reported on fluorescence chemosensors based on 1,8-naphthalimide derivatives for anion and molecular recognition based upon the PET mechanism of 4-amino substitution. The efficiency of PET and ICT processes in amino derivatives of 1,8-naphthalimides has been indicated based on changes in charge density at the 4-amino position with corresponding electron donors [30]. Further, excimer formation processes have been observed in parent chromophores [31-34], with a few studies exploring excimer formation in bis(1,8-naphthalimide) structures [35-37].

In this work, we have designed and developed a novel bifluorogenic probe, Bis[N-ethylglycinate-1,8-naphthalimide] diaza-18-crown-6 (BNDA), featuring two naphthalimide rings linked by an aza crown ether spacer through nitrogen atoms at the 4-position of the naphthalimide rings. This innovative fluorogenic probe, based on ICT and excimer/monomer emission switching, was developed for copper ion detection. The study inspected selectivity, switching emission, and electron transfer signals upon metal ion binding.

2. Experimental

2.1. Materials and instrumentation

Reagent-grade 4-bromo-1,8-naphthalic anhydride, triethylamine, and ethyl glycinate were acquired from Merck and applied as received without further purification. Stock solutions of various metal ions were prepared through dissolving their nitrate and chloride salts in distilled water at a concentration of 0.1 M. UV-Vis spectrophotometric analyses of the dye were performed using a CECIL CE9200 spectrophotometer, with fluorescence measurements conducted with a Perkin-Elmer LS 55 spectrometer.

2.2. General method for spectral measurements

A stock solution of **BNDA** (1.0×10^{-3} M) was prepared in CH_3CN(AN). The fluorescence and Uv-Vis studies on **BNDA** were carried out with (5×10^{-6} M **BNDA**) in (AN-H_2O,1/1, v/v, pH=7). The effect of the metal ions upon the emission intensity was examined through adding adequate amounts of the metal ions to a known volume of the **BNDA**.

2.3. Sample preparation

Synthetic Water Samples: They were prepared by adding 4 µL of solution $Cu(NO_3)_2{\cdot}3H_2O$ (0.1 M), 5 µL each of KNO_3, $NaNO_3$, $CaCl_2$, $3H_2O$, Fe $(NO_3)_3$, $9H_2O_2$ to a 10 mL volumetric flask and diluting with distilled water. For the sensing method, 1 mL of 0.1 M interfere ions was transferred to a 10 mL volumetric flask, after which 50 µL of stock solution of BNDA was added, and diluted with phosphate buffer (pH=7 H_2O:AN 1:1).

Tap Water: It was collected from the Lavizan area in northeast Tehran, filtered, and utilized without further treatment. Next, 1 mL of this water was transferred to a 10 mL volumetric flask, which was followed by adding 50 µL of stock solution of BNDA, and the volume was adjusted to the mark with phosphate buffer (pH=7 H_2O:AN, 1/1, V/V).

Tea Sample: A sample of Persian black tea was purchased from the market. Specifically, 0.2 g of dry black tea was ground into a fine powder and extracted with doubly distilled water under mild stirring at 50°C for four hours. Next, 1 mL of this tea extract was transferred to a 10 mL volumetric flask, after which 50 µL of stock solution of BNDA was added, and the volume was adjusted to the mark with phosphate buffer (pH=7 H_2O:AN, 1/1, V/V).

Hair sample: Pretreatment of hair samples was performed based on wet ashing of human hair. The hair samples were rinsed with acetone; next, the dried samples were weighed and burned in a furnace at 700 °C until a white powder was obtained. The obtained ash was dissolved in a minimum volume of concen-trated HNO_3 with heating to expel brown fumes, and then cooled and diluted with distilled water. Thereafter, 1 mL of this solution was transferred to a 10 mL volumetric flask, whereby 50 µL **A** was added and diluted to the mark with **B**. For the AAS method, the prepared solutions were directly used.

2.4. Synthesis

2.4.1. Synthesis of intermediates (1 and 2)

The synthesis of BNDA and its intermediates is displayed in Scheme 1. According to literature methods, the intermediate compound 1 was synthesized from acenaphthene [38]. A solution of N-Bromo succinimide (0.1 M) was added to acenaphthene (0.1 M) in DMF, and stirred at room temperature for two hours. Subsequently, the participants were filtered from cold water suspension. 4-bromoacenaphthene, yielding 80% was obtained through recrystallization from ethanol with a melting point of 51-52 °C.

Compound 4-bromoacenaphthene (**2**) (8.89 g) was oxidized with glacial acetic acid (155 mL) and sodium dichromate (26.6 g) under reflux. Once cooled down to room temperature, a yellow solid was filtered from queues media. The obtained solid was alkalized at 50°C, then filtered and neutralized with hydrochloric acid. Then purified through recrystallisation in conc. nitric acid, white crystals obtained with a purity of 36 %. Mp: 217 - 220 °C.

2.4.2. Synthesis of N-ethylglycinate-4-bromo-1,8-naphthalimide (3)

N-Ethylglycinate-4-bromo-1,8-naphthalic anhydride (3) was obtained in 90 % yield through condensing 0.01 mol of compound 2 with ethyl glycinate (0.01 mol) in ethanol for four hours. The resultant suspension was poured into 100 mL water, and the precipitated solid filtered off, and further recrystallized with ethanol. The crude product was purified via silica gel column chromatography with acetone as eluant.

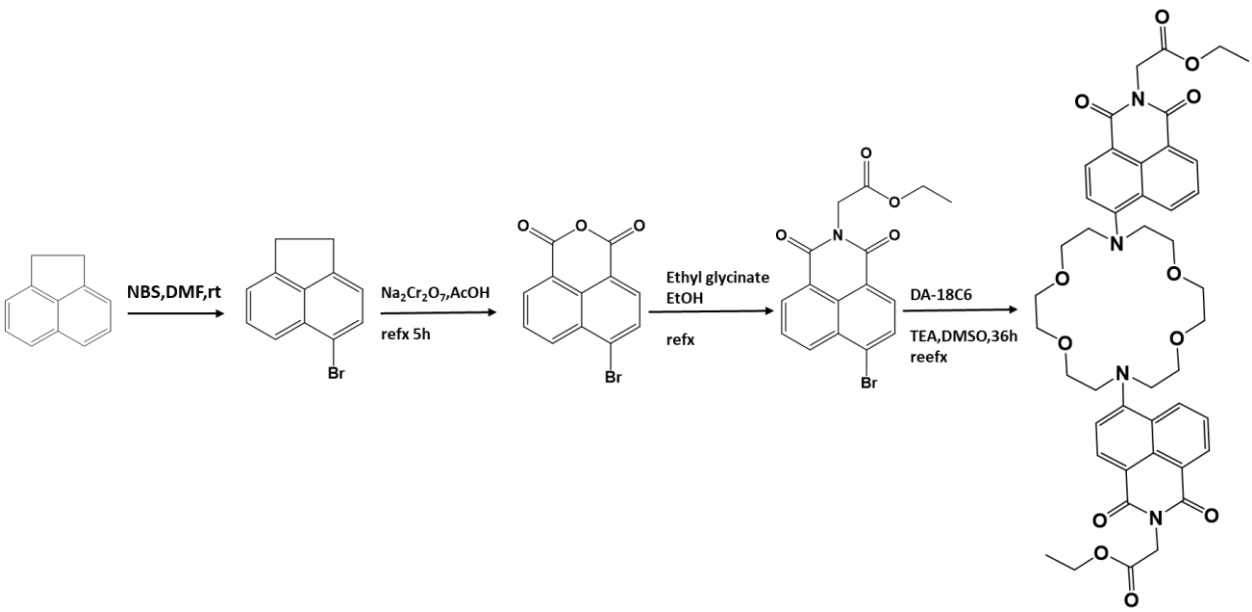

Scheme 1: Synthesis of intermediates and BNDA.

2.4.3. Synthesis of bis[N-ethylglycinate-1,8-naphthalimide] diaza-18-crown-6 (BNDA)

The synthesis of BNDA involved condensing 2 equivalents of N-ethylglycinate-4-bromo-1,8-naphthalimide (3) (0.2 M) with 1 equivalent of diaza-18-crown-6 (0.1 M) in 15 mL of hot DMSO with triethylamine (0.2 M) for 36 hours with stirring. Once cooled down to the room temperature, the product was purified by silica gel plates using dichloromethane: ethyl acetate (40:1) as solvent, yielding pure yellow crystals of BNDA with 30 % yield.

3. Results and Discussion

3.1 Design and synthesis of fluorogenic dye (BNDA)

1,8-Naphthalimides present strong fluorescence when an electron-donating group is substituted at the C-4 or C-5 position. This is owing to the electron pull-push interactions between substituents at the C-4 position and the carbonyl groups in the system, influencing fluorescence efficiency. We introduced ethyl glycinate as a withdrawing substituent at the anhydride ring position of naphthalimide to enhance pull-push characteristics, leading to high sensitivity. The selective interaction of crown ethers with metal ions depends on the type and size of the ions as well as their heteroatoms. The designed fluorogenic dye, based on two N-ethylglycinate-1,8-naphthalimide rings connected via a diaza-18-crown-6 bridge at the amino group of the naphthalimide ring (Scheme 1), revealed significant promise.

3.1.1. Synthesis of 4-bromo-1,8-naphthalic anhydride intermediate (2)

^{1}H-NMR (500 MHz, DMSO-d6): δ (ppm) 8.66 (d, J = 8.66 Hz, 1H), 8.62 (d, J = 7.35 Hz, 1H), 8.39 (d, J = 7.8 Hz, 1H), 8.28 (d, J = 7.85 Hz, 1H), 8.05 (t, J = 7.85 Hz, 1H).

3.1.2. Synthesis of N-ethylglycinate-4-bromo-1,8-naphthalimide (3)

Yield 90 % as a pale-yellow solid, mp=154.57 °C (scheme 1). FTIR (KBr), ν (cm^{-1}): (C-H str. aromatic); 2975 (C-H str. aliphatic); 1743 (C=O str. ester); 1704, 1662 (C=O str. carbonyl); 1584, 1504 (C=C str. aromatic); 1253 (C-O str. ester); 564 (C-Br str). ^{1}HNMR (500 MHz, DMSO-d6): 8.60-7.66 (5H, m, aromatic ring), 4.22 (2H, m, CH_2CH_3), 4.17 (2H, t, $COCH_2$), 2.7(2H, t, -N-CH_2) 1.22 (3H, t, CH_3). Elemental analysis: Calculated for $C_{16}H_{14}NO_4Br$ (Mw 364) C, 52.57; H, 3.85; N, 3.85%: Found C, 52.90; H, 3.78; N, 3.81 %.

3.1.3 Synthesis of bis[N-ethylglycinate-1,8-naphthalimide] diaza-18-crown-6 (BNDA)

Yield 30%, mp=141.55 °C. FTIR (KBr), ν (cm^{-1}): 3090 (C-H Ar.), 2926 (C-H str.), 1743 (C=O str.), 1704, 1662 (C=O str.), 1588, 1507 (C=C str.), 1376 (C-N str.), 1211 (C-O str.). ^{1}HNMR (500 MHz, DMSO-d6) δ: 8.60-7.66 (10H, m, naphthalimide ring), 4.81(4H, m, >N- CH_2), 4.17 (4H, t, -CH_2-O-C=O), 3.71(8H, t, CH_2-O), 3.47(8H, t,-N-CH_2 crown ring), 2.75(8H, t, O-CH_2-CH_2-O), 2.09 (4H, t, -CH_2C=O), 1.15 (6H, t, CH_3). ^{13}CNMR (100 MHz, DMSO-d6) δ: 168.3, 163.0, 151.6, 148.2, 133.8, 132.6, 132.1, 131.9, 131.4, 130.4, 129.5, 127.8, 122.5, 121.7, 31.14, 28.8, 22.8 and 14.5. Ms: m/z$(MH)^+$ 824. Elemental analysis: Calculated for $C_{44}H_{48}N_4O_{12}$ (Mw 824.33) C, 64.08; H, 5.82; N, 6.80%: Found C, 64.11; H, 5.89; N, 6.92 %.

3.2. Spectroscopic properties

The spectroscopic properties of 1,8-naphthalimides are heavily influenced by the molecule's polarity. This molecular polarization depends on the electron-rich or electron-deficient deficiency between the substituent at the C-4 position and the carbonyl groups of the imide in the naphthalimide system. In designing the new fluorophore BNDA, we combined the intramolecular charge transfer (ICT) phenomenon at the naphthalimide ring based on the host-guest interaction of the crown ether molecule with metal ions. In BNDA, the two amino groups of diaza-18-crown-6 are attached at the 4-position of the naphthalimide ring. They serve as electron donors, facilitating an electron transfer process from the non-bonding electrons of the nitrogen groups toward the electron-withdrawing carbonyl groups of the naphthalimide rings. Crown ethers indicate selective bonding to metal ions based on the affinity of their heteroatoms as well as the radius of the metal ions. When a metal ion binds, its positive charge lowers the electron density on the coordinating nitrogen atom, potentially altering the optical properties of the fluorescent molecule and affecting the ICT process [3].

The absorption spectrum of BNDA presents three absorption bands at λ_{max}=237, 343 and 391 nm, which

are related to the E_1, E_2, and B charge-transfer bands of aromatic rings, respectively, with an extinction coefficient (ε) of 6993 (Figure 1). Table 1 reports the spectral characteristics of diaza-18-crown-6 ether functionalized 1,8-naphthalimide in acetonitrile solution, including the absorption maxima (λ_A) and fluorescence emission (λ_F) maxima, the extinction coefficient (log ε), Stokes's shift (ν_A–ν_B), oscillator strength (*f*), quantum yield of fluorescence (ϕ_F), as well as energy yield of fluorescence (EF). BNDA reveals an absorption maximum at λ_{abs}=391 nm. The blue-green fluorescence observed in acetonitrile solution stems from charge transfer from the nitrogen group at the C-4 position to the carbonyl groups. The emission bond shifted to the visible region with maxima at λ_{em}=479 nm.

3.3. pH effect

The influence of pH on BNDA was examined in a solution of acetonitrile and water (AN-H_2O, 1/1, v/v) across a pH range of 2 to 12. The emission behavior of free BNDA by pH in the presence and absence of Cu^{2+} ions is depicted in Figure 2. In acidic conditions, the fluorescence emission of free BNDA is somewhat dependent on pH, with a noticeable enhancement within the pH range of 2.5 to 4. This enhancement is owing to the protonation of the amine group at the 4-position of the naphthalimide ring, which heightens the receptor's oxidation potential and disrupts the PET or ICT thermodynamic pathway. Minimal changes are observed within the pH range of 4.5 to 9.4, suggesting that BNDA is relatively stable within this range. Nevertheless, as the pH rises, the fluorescence intensity of the probe significantly diminishes between pH 9.0 and 11. This reduction is likely due to the deprotonation of the nitrogen group at the four positions of the naphthalimide ring and the hydroxyl groups of the crown ether, which are critical for charge transfer mechanisms of ICT or PET, resulting in fluorescence quenching. Under high acidic conditions in the presence of Cu^{2+} ions, BNDA is fully protonated. Elevation of pH causes deprotonation of BNDA at pH=4 and higher, whereby amine and hydroxyl groups are partially deprotonated and form the BNDA-Cu complex. However, at pH>7, copper ions start to form

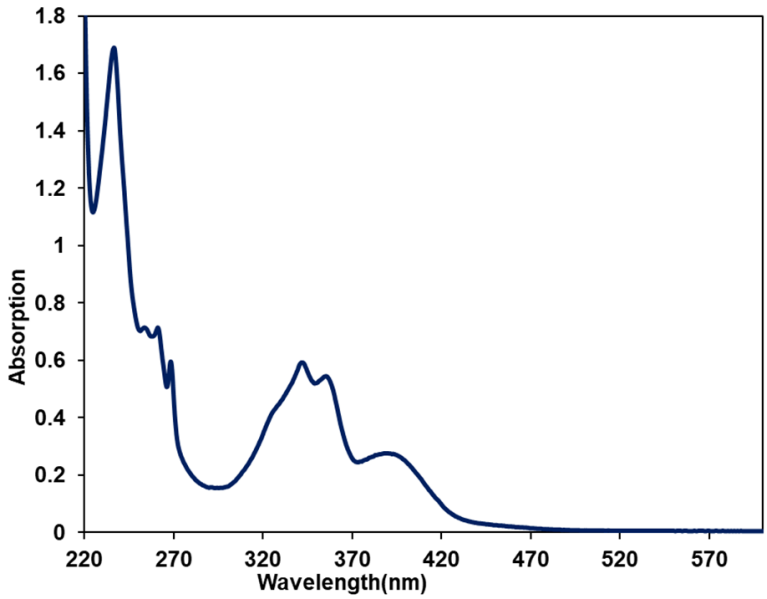

Figure 1: Absorption spectra of BNDA (AN-H_2O,1/1, v/v, pH=7).

Table 1: Photophysical characteristic of BNDA (5.0×10^{-6} M, AN-H_2O,1/1, v/v, pH=7).

compound	λ_{abs} (nm)	λ_{em} (nm)	Logε (l mol^{-1} cm^{-1})	ν_A–ν_B (cm^{-1})	*f*	ϕ_F	E_F
BNDA	237, 343, 391	479	3.844	4698	0.0793	0.1217	0.099

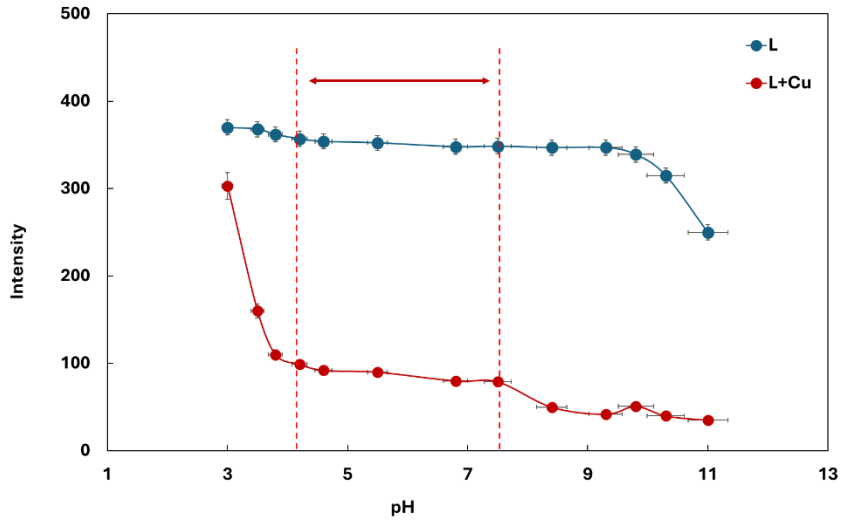

Figure 2: Effect of pH on the emission intensity of BNDA and BNDA-Cu (5.0×10^{-6} M, AN-H_2O,1/1, v/v).

Cu $(OH)_2$. Thus, there is an intensity change and a resulting decline in intensity related to the free BNDA in an alkali medium. The results indicate that BNDA remains stable over a broad pH range of 4.2 to 7.5, making it suitable for use as a fluorescent chemosensor. A pH of 7 was selected for the entire study.

3.4. Selectivity

Initial experiments appraised the interaction of BNDA with various metal ions using spectrofluorimetry in a solution of acetonitrile and water (AN-H_2O, 1/1, v/v, pH=7) at room temperature. In order to observe the behavior of fluorescence spectra of BNDA in the presence of 50 equivalents of metal ions, 15 solutions were prepared from metal ion stock solutions. The fluorescence intensities were recorded at λ_{ex}=391 nm. Figure 3b exhibits the effects of all metal ions.

All metal ions, except for Cu^{2+}, Co^{2+}, Ni^{2+}, Cr^{3+}, and Fe^{3+}, caused a slight augmentation in fluorescence upon addition. In the presence of Cu^{2+}, the intensity of BNDA reveals significant quenching at 479 nm (λ_{ex}=391 nm) with a small red shift (19 nm) (Figure 3c), attributed to the formation of a BNDA–Cu^{2+} complex. The coordination between Cu^{2+} and the diaza-18-crown-6 macrocycle may lower the electron-donating ability of the amino group on the naphthalene ring through the ICT process, leading to fluorescence quenching.

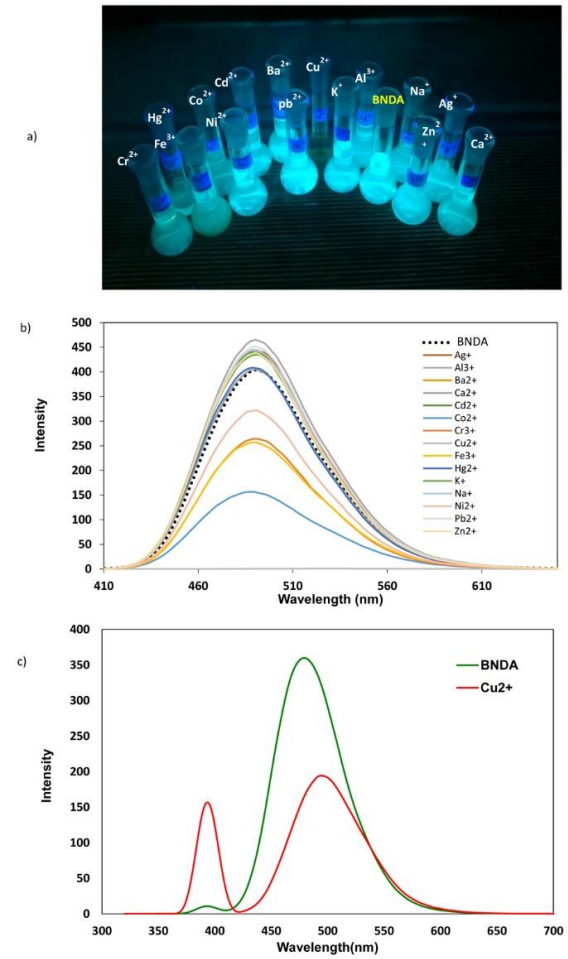

Figure 3: a) Photograph of BNDA (5.0×10^{-6} M, AN-H_2O,1/1, v/v, pH=7) in the presence of 50 equivalent metal ions under UV light (456 nm). b) Fluorescence spectra of BNDA in the presence of 50 equivalent M^{2+}, c). Fluorescence emission spectra (λ_{ex}= 391 nm) of BNDA in the presence of 2 equivalent Cu^{2+}.

The incorporation of the ionophore moiety by Cu^{2+} ions alter the intensity and position of the fluorescence spectrum. This change in emission spectra upon the Cu^{2+} addition suggests that the formation of a BNDA–Cu^{2+} complex disrupts the ICT between the nitrogen atoms on the diaza-18-crown-6 macrocycle and the naphthalimide moiety. These electronic transitions allow BNDA to serve as a sensitive chemosensor for Cu^{2+} detection. The quenching efficiency of metal ions is contingent upon the metal ion and the cavity size as well as affinity of the heteroatoms of the aza crown moiety. A dynamic-static equilibrium excimer emission was reported for parent fluorophores that have fused aromatic rings, such as pyrene and naphthalimide. The formation of excimer in such structures is the outcome of the π-π interactions, which involve an approximate distance (3-4 Å), along with parallel orientation of two aromatic face-to-face ring units [39]. The observed dynamic excimer configuration seems to be due to the naphthalimide dimer formation in the excited state, as previously reported at polar solvents [35]. Nevertheless, in the presence of copper ions, a static excimer emission appears from a naphthalimide dimer in the ground state. The formation of the naphthalimide static excimer is owing to its binding with Cu^{2+}, which was reported to cause the red-shifted excitation spectrum compared to that of the free fluorophore [36].

As expected for parent bichromophoric ionophore structures, the conformational changes are because of metal ion binding of monomer/excimer forms, leading to the fluorophore's different ground or excited state with spectral shifting [35]. Thus, further titration experiments are conducted to explore the binding mechanism between BNDA and Cu^{2+}. 5mL solution D was titrated through adding 1 µL solution of C1 each time, mixed and transferred to a quartz cell, with the fluorescence intensity measured further. Figure 4 demonstrates the fluorescence emission spectra of BNDA (5.0×10^{-6} M) in the presence of different amounts of Cu^{2+}. As displayed in Figure 4, with the gradual addition of Cu^{2+}, the excimer emission band at 479 nm diminishes while the monomer emission band at 392 nm grows. A clear isosbestic point at 420 nm confirms the excimer formation and switching between two monomer/excimer forms by metal ion binding.

The stoichiometry of the complexation of Cu^{2+} with BNDA was determined based on the method of continuous variations (Job's method). Job's plot was obtained through recording the variation in fluorescence intensity (λ_{ex}=391 nm) at 479 nm for a total molar concentration of 1.0 µM. Figure S6 indicates a maximum near 0.5, which can be attributed to the existence of 1:1 BNDA: Cu^{2+}. Further, the binding constant (K_b) of BNDA, a critical parameter in determining the performance efficiency of a synthesized compound as a chemosensor, was calculated by 1:1 stoichiometry using the Benesi-Hildebrand equation (Figure S7). The large K_b of BNDA for Cu^{2+} ions (5.57×10^6 M^{-1}) further confirms the existence of strong coordination in the BNDA - Cu^{2+} complex. The detection of limit (LOD) towards Cu^{2+} was calculated by the following equation (Eq. 1):

$$LOD= 3\sigma/S \quad (1)$$

where σ denotes the standard deviation for the blank solution (5 blank fluorescence measurements); S represents the slope derived from the linear calibration plot; BNDA indicates the linear response range of 2.9×10^{-4} - 4 µM concerning Cu^{2+} ions at low concentrations with a low detection limit (LOD) of 29 nM with LOQ = 87 nM (Figure 4 insets for five replicates with RSD 4.7 %), the slope of 4.95 and R^2=0.995.

Reversibility and stability of probe response are significant factors for the potential application of the probe in real sample analysis. Figure 5 reveals the reversibility of BNDA (5.0×10^{-6} M/AN: H_2O, 1:1) in the presence of 0.2 µM copper ion and adding the 0.2 µM EDTA. Formation of the EDTA-Cu complex releases BNDA, with fluorescence enhancement observed in excimer emission wavelength 479 nm, while emission at monomer wavelength 392 nm drops. Response stability of the probe is another important factor. Figure 5 (inset) demonstrates the BNDA's response with time. The probe's response is stable for 30 min with a relative standard deviation of less than 0.2. The response time is defined as the time required for 95% of the total signal change. It reveals a typical response for the transition process owing to a change in the copper ion concentration. Note that the signal levelled off after equilibrium, with no drift observed in the response time. As can be seen, the response time of the sensor was measured as 30 seconds (Figure S8).

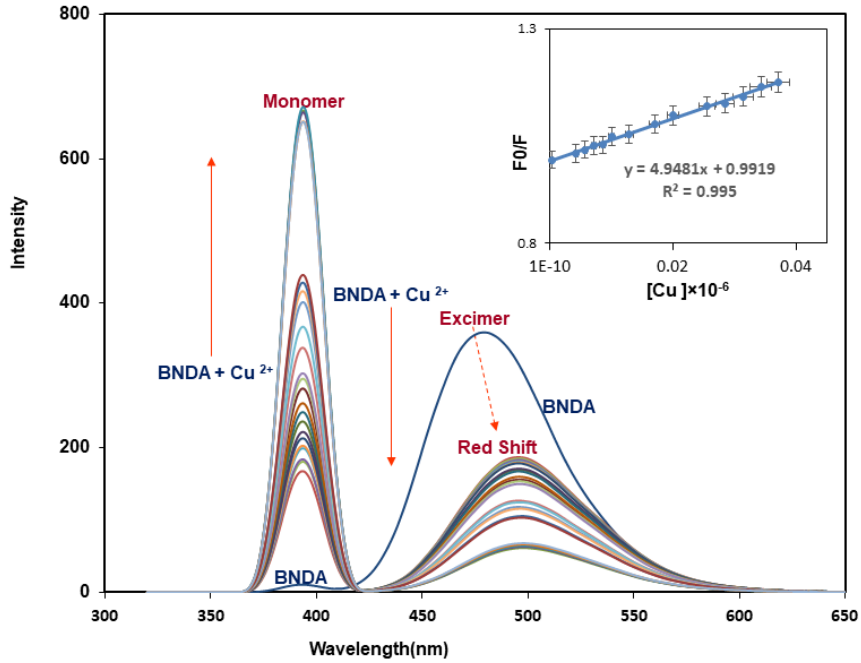

Figure 4: Fluorescence emission spectra of BNDA (5.0×10^{-6} M, AN-H_2O,1/1, v/v, pH=7) in the presence of various concentrations of Cu^{2+} (0-25 equivalent, AN-H_2O,1/1, v/v, pH=7), Inset: Plots of relative intensity at 479 nm versus the Cu^{2+} concentration.

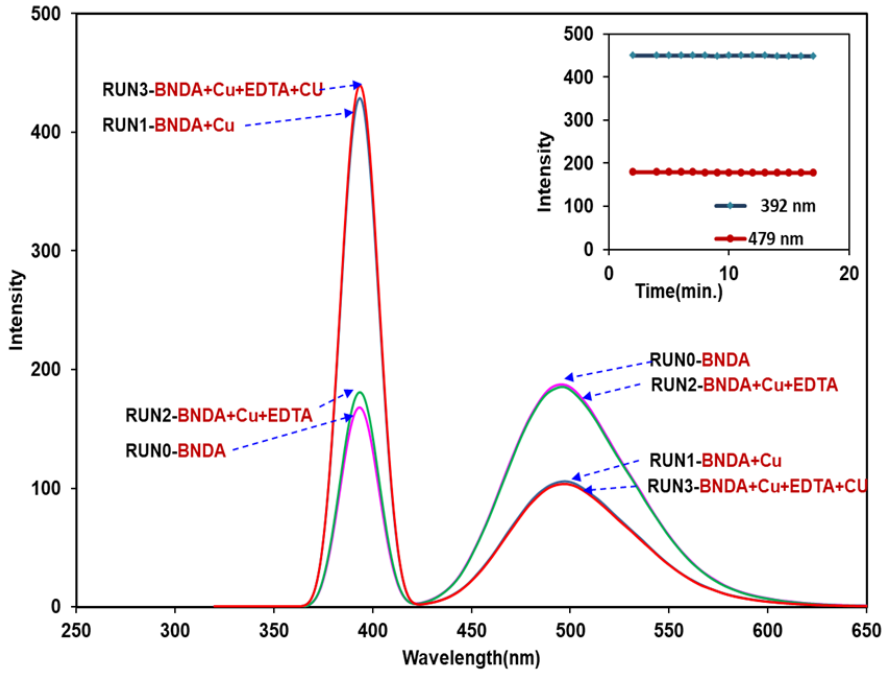

Figure 5: Fluorescence emission of BNDA (5.0×10^{-6}, AN-H_2O,1/1, v/v, pH=7), BNDA+ Cu (0.2μM), BNDA+ Cu (0.2μM)+EDTA (0.2μM), BNDA+ Cu (0.2μM)+ EDTA (0.2μM)+ Cu(0.2μM), inset) Time course of BNDA emission at 392 and 479 nm.

To explore the effect of metal ions on BNDA switching behavior, additional equivalents of copper ions were added. Titration of BNDA with Cu^{2+} revealed that the addition of 1 equivalent of Cu^{2+} (BNDA: Cu^{2+}, 1:1) did not alter the position of the excimer peak (479 nm), but the intensity dropped gradually. Figure 6 depicts the fluorescence intensity changes along the titration of BNDA with Cu^{2+} at the

maximum wavelengths of monomer and excimer. Notably, titration with more than two equivalents of copper ions caused a significant growth in monomer emission (392 nm). The gradient change during titration is evident, with the linear slope of monomer/ excimer changing from 0.5 (BNDA: Cu^{2+}, 1:2 and 1:3) to 0.1 (more than >3 equivalents).

The selectivity of BNDA in aqueous media was researched through adding 100 equivalents of various metal ions to a BNDA solution (5×10^{-6} M) in the absence and presence of 10 equivalents of Cu^{2+} (AN: H_2O, 1:1, v/v). Figure 7 displays the selective sensing of BNDA towards Cu^{2+} over other metal ions. While adding 100 equivalents of various metal ions to the BNDA solution, no significant emission change at 479 nm was observed, except for Cu^{2+}. As illustrated in Figures 3 and 7, Cu^{2+}, Fe^{3+}, Ni^{2+}, Cr^{3+}, and especially Co^{2+} ions can quench BNDA emission, so it is advisable to apply a masking agent for real sample analysis.

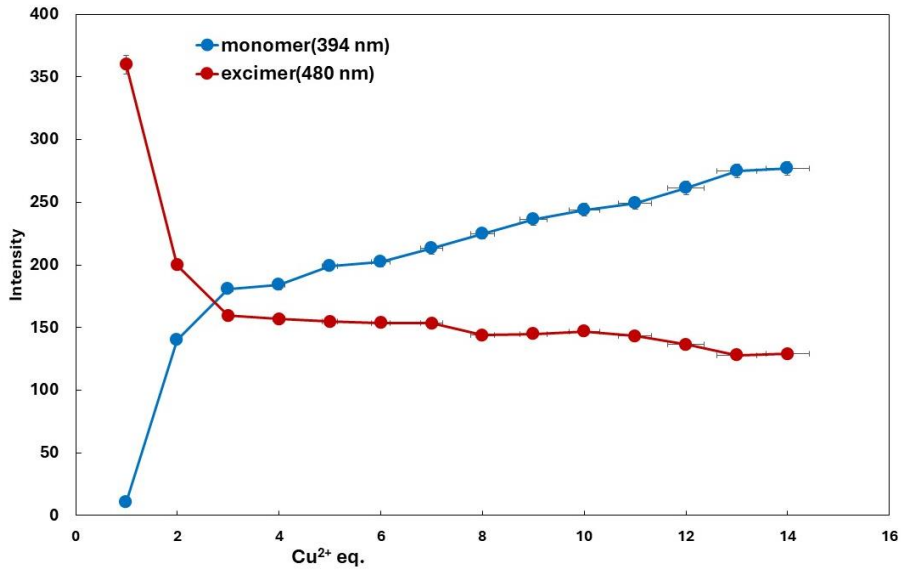

Figure 6: Fluorescence intensity changes along the titration of (5.0×10^{-6}, AN-H_2O,1/1, v/v, pH=7) with Cu^{2+}. (λ_{ex} = 391 nm), emission at 392 nm is for the monomer and 479 nm for excimer.

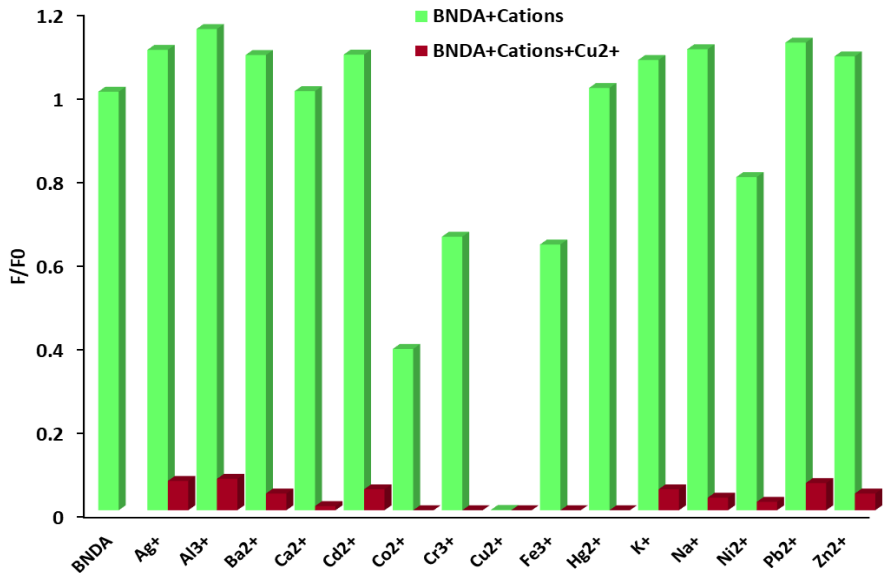

Figure 7: Emission spectra of BNDA (5.0×10^{-6} M, AN-H_2O,1/1, v/v, pH=7) in the presence of 100 eq. of various metal ions and 10 equiv. of Cu^{2+} at maximum excimer emission 479 nm.

Table 2: The real sample analysis results.

Sample	Cu^{2+} added	Cu^{2+} found Atomic absorption	Cu^{2+} found This probe	Recovery %	RSD [a]% (n=8)
Synthetic water	4.00 (µM)	3.94±0.22 (µM)	4.10±0.02 (µM)	102.5	2.43
Tap Water	4.00 (µM)	4.22±035 (µM)	4.15±0.02 (µM)	103.75	2.51
Black tea	-	19.68±0.41 (µg /g)	21.05±0.04 (µg/g)	106.96[b]	3.11
Human hair	-	17.75 ± 0.72 (µg /g)	18.44±0.61 (µg/g)	103.88[b]	2.26

[a] Solvent: **BNDA** (5.0×10^{-6} M, AN-H_2O,1/1, v/v, pH=7), RSD: relative standard deviation

[b] Recovery percent is based on results of atomic adsorption and probe data

3.5. Analytical application

The applicability of the proposed probe was tested through determining copper ion content in samples of tap water, black tea, and human hair. The accuracy of the measurements was compared through atomic absorption analysis, as summarized in Table 2. Using the calibration curve, the copper content in the samples was obtained from n=8 measurements. The results were satisfactory, suggesting that the method was successfully applied.

4. Conclusion

A novel fluorescence dye was introduced based on parent chromophores of naphthalimide rings attached to an aza crown ether spacer. Nitrogen and hydroxyl groups of crown ring as well as esteric groups of imide rings of naphthalimide showed affinity for biding to metal ion. The results indicated formation of eximer configuration in the presence of metal ion binding resulted enhancement of bichromophore emission system with a π-π stacking energy transfer. A dual ON-OFF/OFF-ON excimer/monomer emission switching probe was developed with selectivity towards Cu^{2+} ions. It exhibited remarkable dual responses: ON-OFF fluorescence quenching and OFF/ON enhancement of excimer/monomer emission bands at two different wavelengths, respectively. Depending on the copper ion concentration, BNDA switched between excimer and monomer states. Dual wavelength analysis could enhance sensitivity of trace analysis. The probe revealed selectivity for copper ions, with a low detection limit of 29 nM and a linear range of 2.9×10^{-4} – 4 µM. Its reversible and stable response makes it suitable for real sample analysis. This probe has been successfully applied to determine copper ions in environmental and biological samples.

Acknowledgments

The authors sincerely thank the Institute for Color Science and Technology for making this investigation possible. The authors would also like to thank Dr. S. Seraj for assistance in spectrofluorimetic analysis.

5. References

1. Lakowicz JR, editor. Principles of fluorescence spectroscopy. Boston, MA: springer US; 2006 Sep 15. https://doi.org/10.1007/978-0-387-46312-4_19
2. Gao YY, He J, Li XH, Li JH, Wu H, Wen T, Li J, Hao GF, Yoon J. Fluorescent chemosensors facilitate the visualization of plant health and their living environment in sustainable agriculture. Chem Soc Rev. 2024; 53(13):6992-7090. https://doi.org/10.1039/ D3CS 00504F.
3. Bojinov V, Georgiev N. Molecular sensors and molecular logic gates. J University Chem Technol Metall. 2011 Mar 1;46(1). https://doi.org/10.1007/ 128_2010_96. 112.
4. Khan J. Synthesis and applications of fluorescent chemosensors: a review. J Fluor. 2024; 34(6):2485-94. https://doi.org/10.1007/s10895-023-03455-1
5. Zhao Y, Mei Y, Sun J, Tian Y. A supramolecular fluorescent chemosensor enabling specific and rapid quantification of norepinephrine dynamics. J Am Chem Soc. 2025; 147(6):5025-34. https://doi.org/10.1039/D3 CS00504F.
6. Gurusamy S, Sankarganesh M, Sathish V, Rajakumar K, Mathavan A. Fluorescence chemosensor for anion recognition, solvatochromism and protein binding studies based on Schiff-base derivative. J Mol Struct. 2024; 1312:138542. https://doi.org/10.1016/j.molstruc. 2024.138542.
7. Zhang K, Tian X, Xu P, Zhu Y, Guang S, Xu H. Multi-ion detection chemosensor based on rhodamine for turn-on fluorescence sensing and bioimaging of Fe^{3+}, Al^{3+}, Cr^{3+}, and Hg^{2+} under different channels.

Spectrochimica Acta Part A: Mol Biomol Spect. 2024; 318:124484. https://doi.org/10.1016/j.saa.2024.124484
8. Mohammad Abu-Taweel G, Alharthi SS, Al-Saidi HM, Babalghith AO, Ibrahim MM, Khan S. Heterocyclic organic compounds as a fluorescent chemosensor for cell imaging applications: a review. Critical Rev Anal Chem. 2024; 54(7):2538-53. https://doi.org/10.1080/10408347.2023.2186695.
9. Chowdhury S, Rooj B, Dutta A, Mandal U. Review on recent advances in metal ions sensing using different fluorescent probes. J Fluor. 2018; 28(4):999-1021. https://doi.org/10.1007/s10895-018-2263-y.
10. Li CR, Yang ZY, Li SL. 1, 8-Naphthalimide derived dual-functioning fluorescent probe for "turn-off" and ratiometric detection of Cu^{2+} based on two distinct mechanisms in different concentration ranges. J Lumines. 2018; 198:327-36. https://doi.org/10.1016/j.jlumin.2018.02.031.
11. Alaei P, Rouhani S, Gharanjig K, Ghasemi J. A new polymerizable fluorescent PET chemosensor of fluoride (F^-) based on naphthalimide–thiourea dye. Spectrochim Acta Part A: Mol Biomol Spect. 2012; 90:85-92. https://doi.org/10.1016/j.saa.2012.01.008.
12. Brewer GJ. Copper in Wilson's and Alzheimer's diseases, copper-lowering therapy in cancer and other diseases, and copper deficiency. In Mol Genetic Nutritional Aspects Major Trace Mineral. 2017;115-129. Academic Press https://doi.org/10.1016/ B978-0-12-802168-2.00010-5.
13. Montes S, Rivera-Mancia S, Diaz-Ruiz A, Tristan-Lopez L, Rios C. Copper and copper proteins in Parkinson's disease. Oxidative Medicine Cellular Longevity. 2014; 2014(1):147251. https://doi.org/10.1155/2014/147251
14. Sowada N, Stiller B, Kubisch C. Increased copper toxicity in Saccharomyces cerevisiae lacking VPS35, a component of the retromer and monogenic Parkinson disease gene in humans. Biochemical and biophysical research communications. 2016; 476(4):528-33. http://dx. doi.org/10.1016/j.bbrc.2016.05.157.
15. Li J, Yim D, Jang WD, Yoon J. Recent progress in the design and applications of fluorescence probes containing crown ethers. Chem Soc Rev. 2017;46 (9):2437-58. https://doi.org/10.1039/C6CS00619A.
16. Sprenger T, Schwarze T, Holdt HJ, Hentsch A, Nazaré M. Benzo-Crown-Ether Functionalized O-BODIPY Probes for Cations–A Selective Fluorescent Probe for Ba^{2+}. Chem A Eur J. 2024; 30(45):e202401928. https://doi.org/10.1002/chem.202401928.
17. Polyakova AS, Panchenko PA, Efremenko AV, Feofanov AV, Fedorov YV, Fedorova OA. A naphthalimide-based fluorescent and colorimetric probe for the detection of mercury (II) ions in aqueous solutions and in living cells. Mendel Commun. 2024; 34(3):418-20. https://doi.org/10.1016/j.mencom.2024.04.034.
18. Hosseinnezhad M, Gharanjig K, Fathi M. Synthesis of an organic dye based on indoline for use in dye-sensitized solar cells. J Color Sci Tech. 2025;19(1):101-112. https://doi.org/10.30509/jcst.2025.167615.1267. [In Persian]
19. Xu H, Xiao Y, Liu YG, Sun W. Research progress on naphthalimide fluorescent probes. Adv Sensor Res. 2024; 3(2):2300032. https://doi.org/10.1002/adsr.202300032.
20. Chen M, Stitt H, Chu R, Kistemaker JC, Wood IA, Burn PL, Gentle IR, Shaw PE. Naphthalimide derivatives as film-based fluorescent sensors for rapid detection of illicit drugs. Adv Sensor Res. 2025; 4(10):e00063. https://doi.org/10.1002/adsr.202500063.
21. Chen M, Li Y, Tian H, Xie D, Zhu Y, Wu Y, Zhang X, Zhu M. A multi-stimuli-responsive fluorescence material based on 1,8-naphthalimide. Luminescence. 2024; 39(8):e4868. https://doi.org/10.1002/bio.4868.
22. Kaur G, Singh I, Tandon N, Tandon R, Bhat AA. 1,8-Naphthalimide-based chemosensors: a promising strategy for detection of metal ions in environmental and biological systems. ChemistrySelect. 2023; 8(44): e202301661. https://doi.org/10.1002/slct.202301661.
23. Nie W, Hu L. Design of 1, 8-naphthalimide-based fluorescent functional molecules for biological application: A review. ChemistrySelect. 2024; 9(3): e202303779. https://doi.org/10.1002/slct.202303779
24. Hosseinnezhad M, Nasiri S, Nutalapati V, Gharanjig K, Arabi AM. A review of the application of organic dyes based on naphthalimide in optical and electrical devices. Prog Color Colorant Coat. 2024; 17(4):417-33. https://doi.org/10.30509/pccc.2024.167247.1267
25. Kaur G, Palta A, Kumar G, Paul K, Singh I. Fluorescent "turn-on" naphthalimide conjugate for the detection of CN− ion with potential applications in real water samples and molecular logic gate. Microchemical J. 2025; 209:112845. https://doi.org/10.1016/j.microc.2025. 112845.
26. Acikgoz O, Abelt C. Use of molecular logic gates for the tuning of chemosensor dynamic range. Molecules. 2024; 29(18):4330. https://doi.org/10.3390/molecules29184330.
27. Chen A, Kong F, Fu ZH, Qin JC. Relay recognition of Cu^{2+} and S^{2-} using naphthalimide-based fluorescent probe and its applications in molecular logic gate and bioimaging. Chem Phys. 2024; 577:112132. https://doi.org/10.1016/j.chemphys.2023.112132.
28. Seraj S, Rouhani S, Ranjbar Z, Esfahani SL. Fructose recognition using novel solid-state electro-optical nanosensor based on boronate-tagged fluorophore modified graphene oxide. Mater Chem Phys. 2021; 270:124842. https://doi.org/10.1016/j.matchemphys.2021.124842
29. 28 Rouhani S, Gharagozlou M. A New reusable mercury-sensitive turn-on nano-chemosensor based on functionalized $CoFe_2O_4@SiO_2$ magnetic nano-composite. https://doi.org/10.30509/pccc.2021.166735.
30. Mahdiani M, Rouhani S, Zahedi P. Synthesis, solvatochromism and fluorescence quenching studies of naphthalene diimide dye by nano graphene oxide. J Fluor. 2023; 33(5):2003-14. https://doi.org/10.1007/s10895- 023-03197-0.

31. Seraj S, Rouhani S. A fluorescence quenching study of naphthalimide dye by graphene: mechanism and thermodynamic properties. J Fluor. 2017;27(5): 1877-83. https://doi.org/10.1007/s10895-017-2126-y.
32. Wang HF, Wu SP. A pyrene-based highly selective turn-on fluorescent sensor for copper (II) ions and its application in living cell imaging. Sensor Actuators B: Chem. 2013;181:743-8. http://dx.doi.org/10.1016/j.snb.2013.01.054.
33. Lederer FJ, Graupner FF, Maerz B, Braun M, Zinth W. Excimer formation in 9, 10-dichloroanthracene–Solutions and crystals. Chem. Phys. 2014; 428:82-9. http://dx.doi.org/10.1016/j.chemphys.2013.11.005.
34. Kollár J, Hrdlovič P, Chmela Š. Spectral properties of bichromophoric pyrene derivatives: Monomer vs. excimer fluorescence. J Photochem Photobiol A: Chem. 2010; 214(1):33-9. http://dx.doi.org/10.1016/j.jphotochem. 2010.06.003.
35. Chatterjee S, Kar S, Lahiri S, Basu S. Steric-controlled excimer formation in naphthalene analogues of chalcone. Spectrochim Acta Part A: Mol Biomol Spect. 2004; 60(8-9):1713-8. http://dx.doi.org/10.1016/j.saa.2003.09.011.
36. Ferreira R, Baleizão C, Muñoz-Molina JM, Berberan-Santos MN, Pischel U. Photophysical study of bis(naphthalimide)-amine conjugates: toward molecular design of excimer emission switching. J Phys Chem A. 2011;115(6):1092-9. https://doi.org/10.1021/jp110470h
37. Xu Z, Yoon J, Spring DR. A selective and ratiometric Cu^{2+} fluorescent probe based on naphthalimide excimer–monomer switching. Chem Commun. 2010; 46(15):2563-5. http://dx.doi.org/10.1016/j.jlumin.2012.07.009.
38. Konstantinova TN, Meallier P, Grabchev I. The synthesis of some 1, 8-naphthalic anhydride derivatives as dyes for polymeric materials. Dye Pigm. 1993; 22(3):191-8. http://dx.doi.org/10.1016/0143-7208(93)87006-Z.

How to cite this article:
Rouhani Sh. A Ratiometric Naphthalimide-Based Fluorescent Chemosensor via Excimer-Monomer Switching for the Sensitive Detection of Copper (II) Ions. Prog Color Colorants Coat. 2027;20(1):1-12. https://doi.org/10.30509/pccc.2026.167724.1473.